

Cationic Distribution in Relation to the Magnetic Properties of New M-Hexaferrites with Planar Magnetic Anisotropy $\text{BaFe}_{12-2x}\text{Ir}_x\text{Me}_x\text{O}_{19}$ ($\text{Me} = \text{Co}, \text{Zn}, x \approx 0.85$ and $x \approx 0.50$)

H. Vincent, E. Brando, and B. Sugg

LMGP (CNRS URA 1109), ENS de Physique de Grenoble, BP 46, 38402 Saint Martin d'Hères Cedex, France

Received February 20, 1995; in revised form May 19, 1995; accepted May 22, 1995

Single crystals of $\text{BaFe}_{12-2x}\text{Ir}_x\text{Me}_x\text{O}_{19}$ with $\text{Me} = \text{Co}, \text{Zn}$ and $0 \leq x \leq 1$ have been prepared by a flux method. Precise crystal structures of substituted compounds (Ir–Co with $x = 0.85$ and Ir–Zn with $x = 0.50$) have been determined by using a four-circle diffractometer, and cation distribution on all crystallographic sites has been refined. Magnetization measurements have been performed on single crystals at room and liquid helium temperatures. Observed magnetic anisotropy is planar, and saturation magnetizations are in good agreement with the cation distributions determined by X-ray diffraction. Magnetic anisotropy change is correlated with the substitutions of Ir for Fe cations on bipyramidal and octahedral sites of the R block, and Me for Fe cations on tetrahedral and bipyramidal sites. © 1995 Academic Press, Inc.

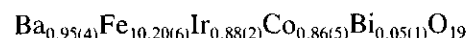
INTRODUCTION

Barium M-hexaferrite has a very strong uniaxial anisotropy; for this reason it is an excellent starting material for permanent magnets. Substituting x (Co–Ti) for $2x$ Fe cations reduces its uniaxial anisotropy, which becomes planar for $x = 1.3$ (1, 2). Co–Ti-substituted M-hexaferrites have been extensively investigated as promising materials for magnetic recording or microwave devices. Unfortunately, the ordering temperature and the saturation magnetization are reduced in proportion to the substitution ratio. Doping barium hexaferrite with Ir–Zn produces the same effects for a much smaller substitution ratio; the magnetic anisotropy becomes planar at only $x = 0.4$ (3). The ordering temperature and saturation magnetization are consequently much higher. Since the work of Tauber *et al.* (3) on Ir–Zn-substituted Ba-hexaferrite many years ago, nothing has been published on this subject to our knowledge. Furthermore, the magnetic properties of Ir^{4+} in dilute solid solutions of ferrimagnetic compounds are rather poorly known. For these reasons it seemed interesting to us to study Ir–Me-doped ($\text{Me} = \text{Co}, \text{Zn}$) barium hexaferrites.

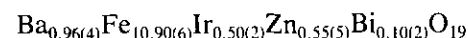
CRYSTAL GROWTH AND CHEMICAL ANALYSIS

Using the technique proposed by Tauber, single crystals were grown from Bi_2O_3 flux in platinum crucibles heated to 1250°C and cooled at 2°C hr^{-1} to 1000°C . BaO_2 or BaCO_3 were used to introduce Ba cations; the molar ratio $\text{Bi}_2\text{O}_3/\text{Fe}_2\text{O}_3$ was approximately 2. Crystals were extracted by hot dilute nitric acid treatment.

Hexagonal platelets up to 3 mm across and 0.5 mm thick were obtained; some small octahedral spinel crystals were present among the hexaferrite platelets. The chemical composition was determined by microprobe analysis. We often noticed Bi present in the analyzed crystals, about 0.05 atoms by formula unit. Normalized in order to have 19 oxygen atoms by formula unit, the average chemical formulae



and



have been found on crystals used for X-ray and magnetic studies. Errors in composition (given in parentheses) have been estimated from the dispersion of measured values at different points of crystals.

STRUCTURE REFINEMENT AND CATION DISTRIBUTIONS

Preliminary precession camera photographs showed cell parameters to be close to those of the undoped M-barium-hexaferrite. They also revealed the same systematic absence of $(h h 2n + 1)$ reflections, confirming the expected isomorphy. Cubic fragments of side about 0.2 mm were extracted from two large crystals and mounted on a Nicolet four-circle diffractometer. About 6350 re-

flections with $\theta \leq 35^\circ$ were collected in half the Ewald sphere, using $\text{MoK}\alpha$ radiation and ω -scan mode.

After Lorentz-polarization corrections, absorption correction, and averaging in the $6/mmm$ Laue class, about 450 independent reflections with $I \geq 3\sigma(I)$ were used in the SHELX refinement program; $\sigma(I)$ is the standard deviation of the measured intensity. The structure was then refined in the $P6_3/mmc$ space group, starting from atomic positions of the undoped M-barium hexaferrite. The weight attributed to each reflection during the refinement was $w = 1/\sigma^2(F_o)$, where $\sigma(F_o)$ was classically defined as in Ref. (4) with a stability factor of 0.02.

In the early stages of refinement, atomic position coordinates, isotropic thermal parameters, and atom population parameters of the Fe sites were refined. All the Fe population parameters except, perhaps, for the tetrahedral Fe3 and octahedral Fe1 sites of the *S* block, were higher than the theoretical population parameters, indicating the presence of Ir cations on all these sites. Therefore, we positioned both Ir and Fe cations on each Fe site, constraining the sum of the atom population parameters to be equal to the theoretical one, and refined again. Under these conditions the crystallographic and weighted *R* factors were $R = 0.043$ and $R_w = 0.056$ in the case of the Ir-Co-substituted ferrite, for instance, but the Fe/Ir thermal parameter of the *2d* bipyramidal site was too large, five times larger than for the other Fe site. Then, we positioned the Fe/Ir cations on the *4e* position with half-occupancy, allowing these cations to be out of the mirror plane in the trigonal bipyramidal site as proposed by some authors (5-7). Thus, the *R* factors became $R = 0.032$ and $R_w = 0.042$, and the Fe2 isotrope thermal parameter became twice those of the other Fe sites.

Microprobe analysis showed the presence of Bi atoms (0.05-0.1 atom by formula unit) in the studied crystals. The Ba multiplicity on site *2d* does not increase when this parameter is refined; thus Bi atoms are located not on this site, but on Fe octahedral sites with Ir atoms. Bi cations (either as Bi^{3+} (8) or as Bi^{5+} cations, as in $\text{Ba}_2\text{LaBiO}_6$ (9)) have been roughly distributed in proportion to the position multiplicities on Fe4 and Fe5 positions and fixed, while the Ir population was refined on each Fe site. After being refined with anisotropic thermal factors, the *R* factors were $R = 0.029$ and $R_w = 0.038$ in the case of the Ir-Co-substituted ferrite, $R = 0.031$, and $R_w = 0.035$ in the case of the Ir-Zn-substituted ferrite.

At this step of the structure refinement, the chemical formulae obtained from the refined site populations were $\text{Ba}(\text{Fe}, \text{Co})_{11.07}\text{Ir}_{0.88}\text{Bi}_{0.05}\text{O}_{19}$ and $\text{Ba}(\text{Fe}, \text{Zn})_{11.47}\text{Ir}_{0.43}\text{Bi}_{0.10}\text{O}_{19}$. The sites occupied by Co^{2+} or Zn^{2+} cations cannot directly be revealed by the structure refinement because of the scattering factor vicinity of Fe, Co, and Zn

TABLE I
Calculated Valencies on Fe Sites

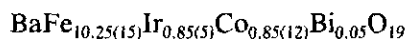
(a) in $\text{BaFe}_{10.25}\text{Ir}_{0.85}\text{Co}_{0.85}\text{Bi}_{0.05}\text{O}_{19}$						
	O1	O2	O3	O4	O5	Valency
Fe1				0.514 (×6)		3.08
Fe2	0.358		0.751 (×3)			2.77
	0.163					
Fe3		0.632		0.658 (×3)		2.60
Fe4			0.427 (×3)		0.568 (×3)	2.99
Fe5	0.520	0.436		0.417 (×2)	0.592 (×2)	2.98
(b) in $\text{BaFe}_{10.90}\text{Ir}_{0.50}\text{Zn}_{0.50}\text{Bi}_{0.10}\text{O}_{19}$						
Fe1				0.514 (×6)		3.08
Fe2	0.361		0.733 (×3)			2.72
	0.160					
Fe3		0.630		0.665 (×3)		2.63
Fe4			0.438 (×3)		0.556 (×3)	2.98
Fe5	0.527	0.435		0.410 (×2)	0.602 (×2)	2.99

atoms. However, the effective valency of each Fe site can be calculated using bond length-bond strength relations on the basis of observed metal-oxygen interatomic distances.

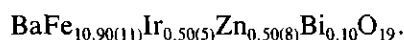
Using the Brown *et al.* relation (10), bond strengths and then effective valencies have been calculated to be

$$s_{ij} = \exp\left(\frac{r_0 - d_{ij}}{0.37}\right),$$

where s_{ij} is the bond strength between bonded atoms *i* and *j*, d_{ij} the bond length, and r_0 a characteristic length; for Fe^{3+} $r_0 = 1.759 \text{ \AA}$ in oxides. The effective valency of the cation *i* is obtained by summing s_{ij} over the *j* first neighbors of the *i* atom. Results are given in Table 1. Valencies of all Fe sites are close to 3.0 except for those of the bipyramidal Fe₂ site (2.77 and 2.72, respectively, for the two hexaferrites) and tetrahedral Fe₃ site (2.60 and 2.62). The presence of Co or Zn atoms has been assumed at these positions. With Co (or Zn) atoms introduced on Fe2 and Fe3 sites proportionally to values estimated from calculated valencies and previously determined Ir populations fixed on each position, the refinement gave the structural parameters of Tables 2 and 4. The final *R* factors are unchanged. Table 3 gives the principal observed interatomic distances. According to these results and their precision, the following chemical formulae are proposed for the studied hexaferrites:



and



MAGNETIC MEASUREMENTS

Magnetization measurements were performed on crystals at room temperature and at low temperatures by using a Foner magnetometer. A Faraday balance was used to determine the ordering temperatures. As shown in Fig. 1, the *c*-axis direction is an easy magnetization direction in nonsubstituted Ba hexaferrite ($x = 0$) and a hard magnetization direction in (Ir-Co)_{0.85}- or (Ir-Zn)_{0.50}-substituted by. As seen in Fig. 1c), the saturation magnetization of the (Ir-Zn)_{0.50}-substituted crystal measured in the (*a*, *b*) plane is reached after a "magnetization rotation progress" (between 1 and 8 kOe). In this compound, the magnetization may lie along a direction situated between the basal plane and the *c*-axis, or stacking defects in the crystals

TABLE 2
Atomic Coordinates ($\times 10^4$) and Equivalent Isotropic
Displacement Coefficients ($\text{\AA}^2 \times 10^4$)

	<i>x</i>	<i>y</i>	<i>z</i>	<i>U</i> (eq)
(a) BaFe _{10.25} Ir _{0.85} Co _{0.85} Bi _{0.05} O ₁₉				
Ba	3,333	6,667	2,500	64 (3)
Fe (1)	0	0	0	40 (6)
Fe (2)	0	0	2,438 (3)	113 (27)
Fe (3)	6667	3,333	2,72 (1)	40 (4)
Fe (4)	6667	3,333	1,905 (1)	30 (3)
Fe (5)	1,680 (1)	3,360 (2)	1,073 (1)	42 (3)
O (1)	0	0	1,515 (4)	14 (10)
O (2)	3,333	6,667	560 (3)	32 (21)
O (3)	8,180 (8)	16,361 (16)	2,500	45 (23)
O (4)	8,447 (6)	16,895 (12)	528 (2)	30 (16)
O (5)	4,974 (7)	9948 (13)	1,500 (2)	20 (13)
(b) BaFe _{10.90} Ir _{0.50} Zn _{0.50} Bi _{0.10} O ₁₉				
Ba	3,333	6,667	2,500	71 (2)
Fe (1)	0	0	0	30 (4)
Fe (2)	0	0	2,566 (2)	101 (11)
Fe (3)	6667	3,333	2,72 (1)	40 (4)
Fe (4)	6667	3,333	1,905 (1)	30 (3)
Fe (5)	1,680 (1)	3,360 (2)	1,073 (1)	42 (3)
O (1)	0	0	1,514 (3)	43 (10)
O (2)	3,333	6,667	560 (2)	30 (10)
O (3)	8,172 (5)	16,343 (10)	2,500	61 (13)
O (4)	8,444 (3)	16,889 (7)	527 (2)	44 (8)
O (5)	4,969 (3)	9939 (7)	1,499 (1)	43 (7)

Note. Equivalent isotropic *U* defined as one-third of the trace of the orthogonalized U_{ij} tensor.

TABLE 3
Bond Lengths Observed on Each
Occupied Polyhedron (\AA)

(a) BaFe _{10.25} Ir _{0.85} Co _{0.85} Bi _{0.05} O ₁₉	
Ba—O (3)	2.955 (1) ($\times 6$)
BaO (5)	2.862 (5) ($\times 6$)
Fe (1)—O (4)	2.004 (4) ($\times 6$)
Fe (2)—O (1)	2.139 (9)
Fe (2)—O (1)	2.429 (9)
Fe (2)—O (3)	1.865 (7) ($\times 3$)
Fe (3)—O (2)	1.929 (6)
Fe (3)—O (4)	1.914 (4) ($\times 3$)
Fe (4)—O (3)	2.074 (4) ($\times 3$)
Fe (4)—O (5)	1.968 (4) ($\times 3$)
Fe (5)—O (1)	2.001 (4)
Fe (5)—O (2)	2.066 (5)
Fe (5)—O (4)	2.083 (5) ($\times 2$)
Fe (5)—O (5)	1.953 (4) ($\times 2$)
(b) BaFe _{10.90} Ir _{0.50} Zn _{0.50} Bi _{0.10} O ₁₉	
Ba—O (3)	2.956 (1) ($\times 6$)
BaO (5)	2.859 (3) ($\times 6$)
and N	
Fe (1)—O (4)	2.005 (3) ($\times 6$)
and N	
Fe (2)—O (1)	2.438 (8)
Fe (2)—O (1)	2.131 (8)
Fe (2)—O (3)	1.876 (5) ($\times 3$)
and N	
Fe (3)—O (2)	1.928 (5)
Fe (3)—O (4)	1.911 (3) ($\times 3$)
and N	
Fe (4)—O (3)	2.063 (4) ($\times 3$)
Fe (4)—O (5)	1.976 (3) ($\times 3$)
and N	
Fe (5)—O (1)	1.997 (3)
Fe (5)—O (2)	2.067 (3)
Fe (5)—O (4)	2.089 (4) ($\times 2$)
Fe (5)—O (5)	1.947 (4) ($\times 2$)

may hinder domain wall displacements. In fact, the magnetic anisotropy becomes planar as early as $x = 0.6$ in the case of the Ir-Co-substituted ferrite (11). Magnetic structure study of these compounds by neutron diffraction, presently in progress, should allow the confirmation of either one or the other of these suppositions. For the $x = 0.85$ substituted Ir-Co hexaferrite and $x = 0.50$ substituted Ir-Zn hexaferrite, ordering temperatures are, respectively, $T_c = 365$ and 362°C . Corresponding saturation magnetizations at $T = 15$ K are $M_s = 86$ emu/g, i.e., $\sigma_s = 18.8 \mu_B$ by formula unit and $M_s = 97$ emu/g, i.e., $\sigma_s = 20.6 \mu_B$ by formula unit.

DISCUSSION

The effective valencies calculated on sites Fe1, Fe4, and Fe5 are close to 3.0 and comparable to those obtained

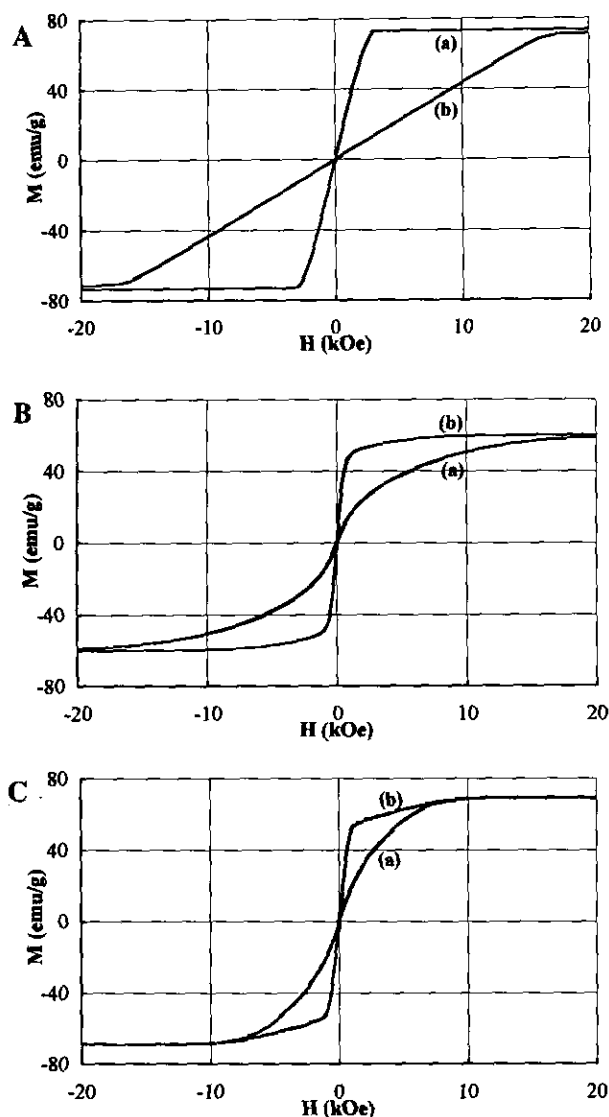


FIG. 1. Magnetization loops versus magnetic field of: (A) $\text{BaFe}_{12}\text{O}_{19}$, (B) $\text{BaFe}_{10.25}\text{Ir}_{0.85}\text{Co}_{0.85}\text{Bi}_{0.05}\text{O}_{19}$, and (C) $\text{BaFe}_{10.90}\text{Ir}_{0.50}\text{Zn}_{0.50}\text{Bi}_{0.10}\text{O}_{19}$; (a) magnetic field along the c -axis, (b) magnetic field perpendicular to the c -axis.

in the nonsubstituted Ba-hexaferrite (5) in spite of the presence of Ir^{4+} cations. This is understandable if one considers the cation size. The effective ionic radii of Fe^{3+} and Ir^{4+} are very similar, 0.645 and 0.625 Å (12); shortening of the interatomic metal–oxygen distance due to a higher Ir^{4+} charge is then impossible. On the other hand, distance lengthening due to lower Co^{2+} charge is of course possible.

The valency calculated on the Fe3 tetrahedral site is very low, 2.60; a larger Co^{2+} amount could be expected at this site, about 0.80 atom instead of the 0.60 value given in Table 4. In fact, as quoted by Wagner and O'Keeffe (13), observed metal–oxygen bonds are longer than nor-

mal on the tetrahedral sites of magnetoplumbite or β -alumina structures; as a result the calculated valency is lower than normal: 2.81 in the nonsubstituted Ba-hexaferrite (5). The calculated valency (2.60) of this site is then probably underestimated.

As can be seen, Ir atoms in the two ferrites are found principally on the octahedral site Fe4(11%) and, when the substitution ratio increases, on the bipyramidal site Fe2 and on the octahedral site Fe5, 10% and 7%, respectively, in the Ir–Co-substituted ferrite. All these sites are neighboring sites. The Fe4 and Fe2 sites belong to the R block and the Fe5 site is located at the R/S block boundary.

All these results agree well with those obtained in Zn–Ti-, Co–Ti-, or Co–Sn-substituted M-hexagonal ferrites. According to Mössbauer spectroscopy studies, the sites substituted by Ti atoms are principally the Fe5, Fe4, and Fe2 sites (14–16). The same sites are usually assumed to be substituted by Co atoms. However, in a recent study by neutron diffraction of substituted Ti–Co M-hexaferrites, Co atoms have been found principally on the Fe3 tetrahedral site and then on the Fe2 bipyramidal site as in this work (17). In fact, this is not surprising, since large bivalent cations ($r \text{Co}^{2+} = 0.58 \text{ \AA}$ compared to $r \text{Fe}^{3+} =$

TABLE 4
Distribution of Cations on Fe Sites; Standard Deviations of Refined Atomic Population Are Given in Parentheses

(a) in $\text{BaFe}_{10.25}\text{Ir}_{0.85}\text{Co}_{0.85}\text{Bi}_{0.05}\text{O}_{19}$						
Site	Position	Fe	Co	Ir	Bi	Spin
Fe1	2 a	0.95(1)		0.05(1) (5%)		Up
Fe2	$\frac{1}{2}(4e)$	0.66(6)	0.25(6) (25%)	0.09(1) (9%)		Up
Fe3	4 f_1	1.35(6)	0.60(6) (30%)	0.05(1) (2.5%)		Down
Fe4	4 f_2	1.77(1)		0.22(1) (11%)	0.01	Down
Fe5	12 k	5.52(1)		0.44(1) (7.5%)	0.04	Up
(b) in $\text{BaFe}_{10.90}\text{Ir}_{0.50}\text{Zn}_{0.50}\text{Bi}_{0.10}\text{O}_{19}$						
Site	Position	Fe	Zn	Ir	Bi	Spin
Fe1	2 a	0.99(1)		0.01(1) (1%)		Up
Fe2	$\frac{1}{2}(4e)$	0.80(4)	0.16(4) (15%)	0.04(1) (4%)		Up
Fe3	4 f_1	1.64(4)	0.34(4) (16.5%)	0.02(1) (1%)		Down
Fe4	4 f_2	1.76(1)		0.21(1) (10.5%)	0.03	Down
Fe5	12 k	5.71(1)		0.22(1) (3.7%)	0.07	Up

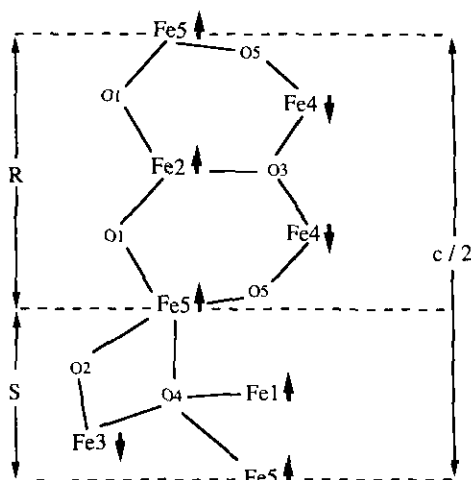


FIG. 2. Scheme of Anderson's magnetic superexchange in the M-hexaferrite.

0.49 Å in tetrahedral coordination (12)) stabilize the spinel block structure and are often found on the spinel tetrahedral site (18). On the other hand, Zn atoms are considered as occupying tetrahedral sites in all the Zn-Ti-substituted hexaferrites because of the very-well-known preference of Zn^{2+} cations for this site. The bipyramidal site, which is preferentially occupied by Co or Zn cations, can be seen also as a pseudo-tetrahedral site because of the off-mirror position of the Fe2 atoms. Our results are therefore consistent.

Figure 2 gives a scheme of superexchange magnetic interactions observed in the M-hexaferrites. $Fe_5-O_4-Fe_1$ and $Fe_5-O_4-Fe_5$ are superexchange interactions with angles close to 90° and so are weak and positive; all other represented superexchange interactions have angles close to 130° and so are strong and negative (19). Thus superexchange interactions lead to the represented magnetic arrangement of Gorter's model (20).

The bipyramidal site Fe2 is considered to play a key role in the axial magneto-crystalline anisotropy of hexaferrites. Preferential substitution of Ir for Fe on octahedral sites Fe4 and Fe5, which are near neighbors of the bipyramidal site, and above all the preferential substitution both of Co (or Zn) and Ir for Fe atoms on the Fe2 site lead naturally to a drastic change in the magnetic anisotropy. The Ti-Co-substituted M-hexaferrite becomes planar for the substitution ratio $x = 1.3$ and the Ir-Co hexaferrite for $x = 0.6$. Unlike Ir^{4+} cations, Ti^{4+} cations never occupy the Fe2 site (17). This is certainly the origin of the much faster change in magnetic anisotropy in Ir-substituted hexaferrites than in Ti-substituted ones.

According to the cation distributions given in Table 4, the calculated saturation magnetizations are $\sigma_c = 18.8 \mu_B$ for $BaFe_{10.25}Ir_{0.85}Co_{0.85}Bi_{0.05}O_{19}$ and $\sigma_c = 20.5 \mu_B$ for

$BaFe_7Ir_{0.50}Zn_{0.50}Bi_{0.10}O_{19}$ by formula unit, very close to the measured values $\sigma_s = 18.8 \mu_B$ and $\sigma_s = 20.6 \mu_B$. In these calculations, the magnetic moments of Fe^{3+} and Co^{2+} cations were considered to be 5 and $3.7 \mu_B$, respectively, and that of Ir^{4+} was considered to be negligible, as found for oxide (21). The $(Ir-Zn)_{0.50}$ -substituted hexaferrite has a saturation magnetization higher than the $(Ir-Co)_{0.85}$ hexaferrite (97 compared to 86 uem/g), but a lower Curie temperature (362 compared to $365^\circ C$). This is understandable since the presence of nonmagnetic Zn cations on tetrahedral sites increases the magnetization but reduces the magnetic interactions of superexchange and then reduces the ferrimagnetic temperature order.

CONCLUSION

Crystal structures of two new M-hexaferrites with x $(Ir-Me)$ -substituted for $2x$ Fe ($Me = Co$ or Zn and $x = 0.85$ or 0.50) have been refined and the Ir and Me cation distribution on Fe sites has been determined. Magnetic properties (order temperature, magnetization versus magnetic field direction) have been studied using single crystals. The basis (a, b) plane is an easy magnetization plane in the substituted hexaferrites. Magnetic anisotropy change seems to be principally correlated with $(Ir-Me)$ -substitution for Fe on the bipyramidal site. Saturation magnetizations measured at low temperature are consistent with those calculated according to the observed cation distribution.

REFERENCES

1. J. Smith and H. P. J. Wijn, "Ferrites," Philips Technical Library, Eindhoven, 1960.
2. H. Kojima, "Ferromagnetic Materials" (E. P. Wohlfarth, Ed.), Vol. 3. North-Holland, Amsterdam, 1982.
3. A. Tauber, J. A. Kohn, and R. O. Savage, *J. Appl. Phys.* **34**, 1265 (1963).
4. G. H. Stout and J. L. Jensen, "X-Ray Structure Determination," 4th ed. MacMillan, New York, 1970.
5. J. G. Rensen, J. A. Schulkes, and J. S. van Wieringen, *J. Phys.* **32**, C1 (1971).
6. J. G. Rensen, J. A. Schulkes, and J. S. van Wieringen, *J. Phys.* **32**, C1 (1971).
7. X. Obradors, A. Collomb, M. Pernet, D. Samaras, and J. C. Joubert, *J. Solid State Chem.* **56**, 171 (1985).
8. D. Le Roux, H. Vincent, J. C. Joubert, and M. Vallet-Regi, *Mater. Res. Bull.* **23**, 299 (1988).
9. P. P. Kiricok, N. B. Voronina, and O. F. Berezak, *Izv. Vyssh. Uchebn. Zaved. Fiz.* **27**, 116 (1984).
10. R. Schulder, *Z. Anorg. Allg. Chem.* **319**, 375 (1963).
11. I. D. Brown and D. Altermatt, *Acta Crystallogr. Sect. B* **41**, 244 (1985).
12. B. Sugg and H. Vincent, *J. Magn. Magn. Mater.*, 139 (1995).
13. R. D. Shannon, *Acta Crystallogr. Sect. A* **32**, 751 (1976).
14. T. R. Wagner and M. O'Keeffe, *J. Solid State Chem.* **73**, 211 (1988).

14. V. F. Belov, T. A. Khimich, M. N. Shipko, I. S. Zheludev, E. V. Korneev, and N. S. Ovanesyan, *Sov. Phys. JETP* **37**(6), 1089 (1973).
15. Y. K. Hong, Y. J. Paig, D. G. Agresti, and T. D. Shelfer, *J. Appl. Phys.* **61**, 3872 (1987).
16. D. H. Han, Z. Yang, H. X. Zeng, X. Z. Zhou, and A. H. Morrish, *J. Magn. Magn. Mater.* **137**, 191 (1994).
17. M. V. Cabanas, J. M. Gonzalez-Calbet, J. Rodriguez-Carjaval, and M. Vallet-Regi, *J. Solid State Chem.* **111**, 229 (1994).
18. B. Kamb, *Am. Mineral.* **53**, 1439 (1968).
19. J. Kanamori, *J. Phys. Chem. Solids* **10**, 87 (1959).
20. E. W. Gorter, *Proc. IEEE* **104**, 225 (1957).
21. "Gmelin Handbuch der Anorganischen Chemie," Vol. 67, p. 5. Springer, Berlin, 1978.